



Published in final edited form as:

J Neurochem. 2013 September ; 126(6): 739–748. doi:10.1111/jnc.12355.

Nesfatin-1 activates cardiac vagal neurons of nucleus ambiguus and elicits bradycardia in conscious rats

G. Cristina Brailoiu¹, Elena Deliu², Andrei A. Tica^{2, #}, Joseph E. Rabinowitz^{2, 3}, Douglas G. Tilley^{2, 3}, Khalid Benamar⁴, Walter J. Koch^{2, 3}, and Eugen Brailoiu^{2, 3, *}

¹Department of Pharmaceutical Sciences, Thomas Jefferson University, Jefferson School of Pharmacy, Philadelphia, PA 19107

²Department of Pharmacology, Temple University School of Medicine, Philadelphia, PA 19140

³Center for Translational Medicine, Temple University School of Medicine, Philadelphia, PA 19140

⁴Center for Substance Abuse Research, Temple University School of Medicine, Philadelphia, PA 19140

Abstract

Nesfatin-1, a peptide whose receptor is yet to be identified, has been involved in the modulation of feeding, stress and metabolic responses. More recently, increasing evidence supports a modulatory role for nesfatin-1 in autonomic and cardiovascular activity. This study was undertaken to test if the expression of nesfatin-1 in the nucleus ambiguus, a key site for parasympathetic cardiac control, may be correlated with a functional role. Since we have previously demonstrated that nesfatin-1 elicits Ca²⁺ signaling in hypothalamic neurons, we first assessed the effect of this peptide on cytosolic Ca²⁺ in cardiac preganglionic neurons of nucleus ambiguus. We provide evidence that nesfatin-1 increases cytosolic Ca²⁺ concentration via a Gi/o-coupled mechanism. The nesfatin-1-induced Ca²⁺ rise is critically dependent on Ca²⁺ influx via P/Q-type voltage-activated Ca²⁺ channels. Repeated administration of nesfatin-1 leads to tachyphylaxis. Further, nesfatin produces a dose-dependent depolarization of cardiac vagal neurons via a Gi/o-coupled mechanism. *In vivo* studies, using telemetric and tail-cuff monitoring of heart rate and blood pressure, indicate that microinjection of nesfatin-1 into the nucleus ambiguus produces bradycardia not accompanied by a change in blood pressure in conscious rats. Taken together, our results identify for the first time that nesfatin-1 decreases heart rate by activating cardiac vagal neurons of nucleus ambiguus.

Keywords

autonomic control; calcium imaging; cardiovascular regulation

*Corresponding author: Eugen Brailoiu, M.D., Department of Pharmacology and Center for Translational Medicine, Temple University School of Medicine, 3500 N. Broad Street, Philadelphia, PA 19140; Tel: 215-707-2791; ebrailou@temple.edu.
#AAT's present address is Department of Pharmacology, School of Medicine, University of Medicine and Pharmacy, Craiova, Romania.

The authors have no conflict of interests.

Introduction

Nesfatin-1, an 82 amino acid cleavage product of nucleobindin-2 protein, has been described as a central and peripheral satiety molecule that induces acute and chronic anorexigenic effects (Oh-I *et al.* 2006, Maejima *et al.* 2009). Its widespread distribution throughout the brain (Brailoiu *et al.* 2007, Goebel *et al.* 2009) and the periphery (Palasz *et al.* 2012) suggests that it may regulate other functions besides feeding. Experimental evidence supports the involvement of nesfatin-1 in the modulation of neuroendocrine functions, stress, metabolic responses (García-Galiano *et al.* 2010, Stengel & Taché, 2011).

With respect to the cardiovascular regulation, nesfatin-1 elevates blood pressure and renal sympathetic nerve activity upon intracerebroventricular administration in conscious and urethane-anesthetized rats (Yosten & Samson 2009, Tanida & Mori 2011). Further, nesfatin-1 modulates the excitability of nucleus of the solitary tract neurons and produces hypertensive and tachycardic responses upon microinjection at this site (Mimee *et al.* 2012). Direct modulation of peripheral arterial resistance also mediates nesfatin-1-dependent pressor effects (Yamawaki *et al.* 2012). Nesfatin-1 expression in the heart has been correlated with negative inotropism and protection against ischemia-reperfusion injury (Angelone *et al.* 2012).

Premotor cardiac vagal neurons of nucleus ambiguus play an essential role in heart rate regulation (Mendelowitz, 1999). Since nesfatin-1 immunoreactivity has been detected in nucleus ambiguus in rodents (Goebel *et al.* 2009, Goebel-Stengel *et al.* 2011), we used *in vitro* and *in vivo* approaches to examine whether or not nesfatin-1 has a functional role in cardiac-projecting neurons of nucleus ambiguus neurons.

Experimental procedures

Chemicals

All chemicals were from Sigma-Aldrich (St. Louis, MO) unless otherwise mentioned.

Animals

Neonatal Sprague-Dawley rats (1–2 days old) (Charles River Laboratories, Wilmington, MA) of either sex were used for retrograde tracing and neuronal culture and adult male rats were used for telemetric and tail-cuff measurement of heart rate. Protocols were reviewed and approved by the Institutional Animal Care and Use Committee.

Neuronal labeling and culture

Preganglionic cardiac vagal neurons of nucleus ambiguus were retrogradely labeled by intrapericardial injection of rhodamine [5(6) X-RITC; X-rhodamine-5-(and-6)-isothiocyanate] 40 µl, 0.01%, (Invitrogen, Carlsbad, CA), as previously reported (Bouairi *et al.* 2006, Brailoiu *et al.* 2012, 2013). Medullary neurons were dissociated and cultured 24 h after rhodamine injection, as described (Brailoiu *et al.* 2012, 2013). Briefly, the brains were quickly removed and immersed in ice-cold Hanks' balanced salt solution (HBSS) (Mediatech, Manassas, VA). The ventral side of the medulla (containing nucleus ambiguus) was dissected, minced, and the cells were dissociated by enzymatic digestion with papain,

followed by mechanical trituration. After centrifugation at 500 g, fractions enriched in neurons were collected and resuspended in culture medium containing Neurobasal-A (Invitrogen), which promotes the survival of postnatal neurons, 1% GlutaMax (Invitrogen), 2% penicillin–streptomycin–amphotericin B solution (Mediatech), and 10% fetal bovine serum (Atlanta Biologicals Inc., Lawrenceville, GA). Cells were plated on round 25 mm glass coverslips previously coated with poly-L-lysine in six-well plates. Cultures were maintained at 37°C in a humidified atmosphere with 5% CO₂. The mitotic inhibitor cytosine β-arabino furanoside (1 μM) was added to the culture to inhibit glial cell proliferation (Schoniger *et al.* 2001).

Calcium imaging

Measurements of [Ca²⁺]_i were performed as previously described (Brailoiu *et al.* 2012, 2013). Cells were incubated with 5 μM fura-2 AM (Invitrogen, Carlsbad, CA) in HBSS at room temperature for 45 min, in the dark, washed three times with dye-free HBSS, and then incubated for another 45 min to allow for complete de-esterification of the dye. Coverslips (25 mm diameter) were subsequently mounted in an open bath chamber (RP-40LP, Warner Instruments, Hamden, CT) on the stage of an inverted microscope Nikon Eclipse TiE (Nikon Inc., Melville, NY). The microscope was equipped with a Perfect Focus System and a Photometrics CoolSnap HQ2 CCD camera (Photometrics, Tucson, AZ). During the experiments the Perfect Focus System was activated. Fura-2 AM fluorescence (emission= 510 nm), following alternate excitation at 340 and 380 nm, was acquired at a frequency of 0.25 Hz. Images were acquired and analyzed using NIS-Elements AR 3.1 software (Nikon Inc.). The ratio of the fluorescence signals (340/380 nm) was converted to Ca²⁺ concentrations (Grynkiewicz *et al.* 1985).

Measurement of membrane potential

The relative changes in membrane potential of single neurons were evaluated using bis-(1,3-dibutylbarbituric acid) trimethine oxonol, DiBAC₄(3) (Invitrogen), a slow response voltage-sensitive dye, as previously described (Brailoiu *et al.* 2010). Upon membrane hyperpolarization, the dye concentrates in the cell membrane, leading to a decrease in fluorescence intensity, while depolarization induces the sequestration of the dye into the cytosol, resulting in an increase of the fluorescence intensity (Brauner *et al.* 1984). Cultured neurons were incubated for 30 min in HBSS containing 0.5 mM DiBAC₄(3) and fluorescence monitored at 0.17 Hz (excitation/emission 480nm/540nm). Calibration of DiBAC₄(3) fluorescence following background subtraction was performed using the Na⁺-K⁺ ionophore gramicidin in Na⁺-free physiological solution and various concentrations of K⁺ (to alter membrane potential) and N-methylglucamine (to maintain osmolarity) (Brauner *et al.* 1984). Under these conditions the membrane potential is approximately equal to the K⁺ equilibrium potential determined by the Nernst equation. The intracellular K⁺ and Na⁺ concentration were assumed to be 130 mM and 10 mM, respectively.

Surgical procedures

Male Sprague-Dawley rats (200–250 g) were anesthetized with an intraperitoneal injection of a mixture of ketamine hydrochloride (100–150 mg/kg) and acepromazine maleate (0.2

mg/kg). Animals were placed into a stereotaxic instrument; a guide C315G cannula (PlasticsOne, Roanoke, VA) was bilaterally inserted into the nucleus ambiguus and fixed in position with dental cement. The stereotaxic coordinates for identification of nucleus ambiguus were: 12.24 mm posterior to bregma, 2.1 mm from the midline and 8.2 mm ventral to the dura mater (Paxinos & Watson, 1998). A C315DC cannula dummy (PlasticsOne) of identical length was inserted into the guide cannula to prevent any contamination. For the implantation of transmitters, an incision 2 cm in length was made along the linea alba, and the underlying tissue was dissected and retracted. A calibrated transmitter (E-mitters, series 4000; Mini Mitter, Sunriver, OR) was inserted in the intraperitoneal space, as previously described (Benamar *et al.* 2010). After the transmitter was passed through the incision, the abdominal musculature and dermis were sutured independently and the animals were returned to individual cages. The animals were observed daily to ensure health and recovery.

Telemetric heart rate monitoring

The signal generated by transmitters was collected via series 4000 receivers (Mini Mitter, Sunriver, OR) placed underneath the home cage. VitalView™ software (Mini Mitter, Sunriver, OR) was used for data acquisition. Each data point represents the average of heart rate per 1 min.

Non-invasive blood pressure measurement

In rats with cannula inserted into the nucleus ambiguus, blood pressure was non-invasively measured by determining the tail blood volume with a volume pressure recording sensor and an occlusion tail-cuff (CODA System, Kent Scientific, Torrington, CT). The nose cone was custom modified to allow access to the cannula. One week after the insertion of the cannula, rats were exposed to handling and training every day for 1 week, starting with 25 minutes in the first day of handling and training in the room where measurements were to be taken and progressively increasing the time to 1 h in the day seven (Fraser *et al.* 2001; Feng *et al.* 2008). The maximum occlusion pressure was 200 mm Hg, minimum volume 30 mm Hg and deflation time 10 seconds. Three measurements were done per minute (one cycle) and the average was used to calculate heart rate, systolic and diastolic blood pressure as well as mean arterial pressure. Ten acclimatization cycles were done before starting the experiments.

Microinjection into nucleus ambiguus

One week after surgery (telemetry studies) or after another week of training (tail-cuff measurements), either vehicle, L-glutamate or nesfatin-1 was bilaterally microinjected into the nucleus ambiguus, using the C315I internal cannula (33 gauge, PlasticsOne), without handling the rats (telemetric measurement). In case of the tail-cuff method, trained rats were in the animal holder for the duration of the experiment. Handling the rats induced a robust increase in heart rate in the absence of any treatments (McDouglas *et al.* 2004). For recovery, at least two hours were allowed between two injections. Injection of L-glutamate (5 mM, 50 nL with Neuros Hamilton syringe, Model 7000.5 KH SYR) was used for the

functional identification of nucleus ambiguus (Chitravanshi *et al.* 2009; Brailoiu *et al.* 2013).

Histology

Typical sites of cannula placement in the nucleus ambiguus were marked by microinjections of diluted (1:42) green Lumafluor retrobeads (Lumafluor Inc., Durham, NC) as previously reported (Brailoiu *et al.* 2013). Rats were perfused and fixed with 4% paraformaldehyde. Serial sections of the medulla were cut (30–40 μm), mounted on slides, covered with Vectashield mounting medium (Vector Laboratories, Burlingame, CA) and coverslipped. The microinjection sites were identified using a fluorescence microscope, photographed and compared with a standard rat brain atlas (Paxinos & Watson, 1998).

Statistical analysis

Data were expressed as mean \pm standard error of mean. One-way ANOVA followed by *post hoc* analysis using Bonferonni and Tukey tests was used to evaluate significant differences between groups.

Results

Nesfatin-1 elevates cytosolic Ca^{2+} in cardiac preganglionic neurons of nucleus ambiguus

Nesfatin-1 (10^{-6}M) produced a robust increase in $[\text{Ca}^{2+}]_i$ in rhodamine-labeled cardiac-projecting neurons of nucleus ambiguus: the Ca^{2+} response was characterized by a fast increase followed by a plateau lasting 2–3 min (Fig. 1A). The nesfatin-1-induced Ca^{2+} response returned to basal levels within 4 min. Nesfatin (10^{-8} , 10^{-7} , 10^{-6} and 10^{-5} M) produced an increase in $[\text{Ca}^{2+}]_i$ by 32 ± 1.7 nM, 271 ± 3.9 nM, 367 ± 4.3 nM, and 376 ± 4.9 nM, respectively ($n = 6$ for each concentration tested) (Fig. 1B); statistical significance ($P < 0.05$) was attained for the higher doses of nesfatin (10^{-7} , 10^{-6} and 10^{-5}M). The increase in $[\text{Ca}^{2+}]_i$ produced by the highest concentration of nesfatin (10^{-5} M) tested was not statistically different from that produced by nesfatin 10^{-6} M (Fig. 1B). Pretreatment with the oxytocin receptor antagonist L-371,257 (10^{-7}M) (Kuo *et al.*, 1998) or with the antagonist of melanocortin receptors type 3/4, SHU 9119 (10^{-7} M) (Tanida & Mori, 2011), did not significantly affect the increase in $[\text{Ca}^{2+}]_i$ produced by nesfatin-1 (10^{-6}M): $[\text{Ca}^{2+}]_i = 376 \pm 4.9$ nM in the absence of the antagonists, vs 358 ± 6.3 nM in the presence of L-371,257 or 349 ± 5.7 nM in the presence of SHU 9119 ($n = 6$ for each treatment) (Fig. 1B).

Repeated administration of nesfatin-1 produces tachyphylaxis

In this series of experiments, cardiac vagal neurons of nucleus ambiguus were treated with nesfatin-1 twice, while monitoring the Ca^{2+} response. The second application of nesfatin-1, after Ca^{2+} returned to the basal values following the first response, produced an increase in $[\text{Ca}^{2+}]_i$ with a lower amplitude than the first application (Fig. 2). Representative images of fluorescence 340/380 ratio of a rhodamine-labeled neuron treated twice with nesfatin-1 (10^{-6} M) are shown in Fig 2A, and examples of individual Ca^{2+} responses after two treatments with nesfatin-1 are shown in Fig. 2C. As illustrated in Fig. 2D, the initial application of nesfatin-1 (10^{-6} M) increased $[\text{Ca}^{2+}]_i$ by 354 ± 4.6 nM ($n = 6$), while the Ca^{2+} response to the subsequent application was significantly reduced to 142 ± 2.8 nM ($P < 0.05$,

n = 6), indicating tachyphylaxis. We have previously shown that urocortin 3 activates nucleus ambiguus neurons (Brailoiu *et al.* 2012). We tested if the response to urocortin 3 was affected by previous treatment with nesfatin-1. When the cells were treated with urocortin 3 after recovering to the basal level after the nesfatin-1 application, the response to urocortin 3 was not affected (Fig. 2B, C) and similar to that previously reported (Brailoiu *et al.* 2012).

Nesfatin-1 effects are mediated by a Gi/o-coupled mechanism in nucleus ambiguus neurons

The Ca²⁺ response of cardiac vagal neurons to nesfatin-1 (10⁻⁶ M) was markedly reduced by inhibition of Gi/o proteins with pertussis toxin (PTX, 100 nM): [Ca²⁺]_i = 38 ± 3.4 nM after pertussis toxin (n = 6, P < 0.05), as compared to [Ca²⁺]_i = 367 ± 4.3 nM, in the absence of the pertussis toxin. On the other hand, incubation with cholera toxin (CTX, 100 nM), that blocks Gs-dependent signaling, did not affect the nesfatin-1 induced increase in [Ca²⁺]_i (3 [Ca²⁺]_i was 367 ± 5.1 nM, n = 6 in presence of CTX vs 367 ± 4.3 nM upon treatment with nesfatin-1 alone) (Fig. 3A, B).

Nesfatin-1-induced Ca²⁺ elevation is contingent on Ca²⁺ influx via voltage-gated P/Q channels

Nesfatin-1(10⁻⁶ M) -induced increase in [Ca²⁺]_i was abolished when cardiac preganglionic neurons of nucleus ambiguus were incubated with Ca²⁺-free saline ([Ca²⁺]_i = 5 ± 1.3 nM, n = 6), indicating that its effect on [Ca²⁺]_i is dependent on Ca²⁺ influx via plasmalemmal Ca²⁺ channels. Using selective Ca²⁺ channels blockers, we evaluated the contribution of different types of voltage-gated Ca²⁺ channels to nesfatin effects. In the presence of nifedipine (1 μM), a L-type Ca²⁺ channel inhibitor, or -conotoxin GVIA (100 nM), a blocker of N-type Ca²⁺ channels, nesfatin-1 (10⁻⁶ M) elevated [Ca²⁺]_i by 359 ± 5.2 nM (n = 6) and 344 ± 4.8 nM (n = 6), respectively, responses largely resembling that produced in absence of any blocker ([Ca²⁺]_i = 367 ± 4.3 nM, Fig. 4A, B). However, preventing Ca²⁺ influx via P/Q-type Ca²⁺ channels with -conotoxin MVIIC (100 nM) basically abolished the effect of nesfatin ([Ca²⁺]_i = 19 ± 2.6 nM, n = 6, Fig. 4A, B).

Nesfatin-1 depolarizes cardiac vagal neurons of nucleus ambiguus

Cultured vagal preganglionic neurons had a mean resting potential of -55.75 ± 0.05 mV (n = 24), as previously reported using classical electrophysiological techniques in brain stem slices (Brailoiu *et al.* 2013) or cultured neurons (Mendelowitz and Kunze, 1991), or by using voltage imaging in cultured neurons (Brailoiu *et al.*, 2012). Administration of nesfatin-1 resulted in a rapid membrane depolarization, which declined gradually and receded within 4 min; a representative recording is shown in Fig. 5A. The effect of nesfatin-1 on membrane potential was sensitive to Gi/o protein blockade with pertussis toxin. Increasing concentrations of nesfatin-1 (10⁻⁸, 10⁻⁷, 10⁻⁶ and 10⁻⁵M) depolarized cardiac preganglionic neurons by 0.51 ± 0.16 mV, 3.97 ± 0.28 mV, 6.34 ± 0.47 mV, and 6.53 ± 0.54 (n = 6 for each concentration), respectively (Fig. 5B). Depolarizations induced by 10⁻⁷, 10⁻⁶ and 10⁻⁵M nesfatin-1 were statistically significant (P < 0.05), as compared to the resting membrane potential. The amplitude of the depolarization induced by the highest

concentration of nesfatin tested (10^{-5} M) was not statistically different from that produced by nesfatin 10^{-6} M ($P > 0.05$). Pretreatment with pertussis toxin (PTX, 100 nM), abolished the depolarization induced by 10^{-6} M nesfatin-1 (0.82 ± 0.63 mV, $n = 6$, Fig. 5B), supporting the Gi/o-dependency of the response.

Microinjection of nesfatin-1 into nucleus ambiguus decreases the heart rate in awake rats

In conscious, freely moving rats, bearing cannula implanted into nucleus ambiguus, microinjection of nesfatin-1 (5 pmol) produced a decrease in heart rate; a representative example is shown in Fig. 6A. Microinjection of L-glutamate (L-Glu, 5 mM) into the nucleus ambiguus elicited a bradycardic response (Fig. 6A) as previously reported, indicating the correct placement of cannula (Chitravanshi *et al.* 2009, 2012; Brailoiu *et al.*, 2013). Microinjection of L-glutamate (5 mM, 50 nl) into the nucleus ambiguus reduced the heart rate by 83 ± 6 beats per minutes ($n = 5$). Microinjection of nesfatin-1 (0.05, 0.5 and 5 pmol), 2 h after L-glutamate, elicited a dose-dependent decrease in heart rate by 7 ± 3 , 29 ± 4 and 41 ± 5 beats per min, respectively ($n = 5$ rats for each dose tested) (Fig. 6B).

To verify whether or not the microinjection of nesfatin-1 in nucleus ambiguus was associated with any change in blood pressure, the blood pressure was monitored by tail-cuff method in rats with a cannula inserted in the nucleus ambiguus after one week of training. Microinjection of L-glutamate and nesfatin-1 into the nucleus ambiguus produced bradycardic responses that were not accompanied by changes in blood pressure; representative examples of recordings are shown in Fig. 6A. Microinjection of L-glutamate (5 mM, 50 nl) decreased the heart rate by 84 ± 4 beats per min and microinjection of nesfatin-1 (5 pmol) decreased the heart rate by 42 ± 4 beats per min ($n = 5$). (Fig. 6B); these values are similar to those obtained by telemetric measurement. The excellent correlation between the two methods is in agreement with previous studies (Fraser *et al.* 2001; Feng *et al.* 2008).

Discussion

Emerging evidence supports a broad range of regulatory roles for nesfatin-1 in addition to the initial reported role on feeding behavior (Oh-I *et al.* 2006; García-Galiano *et al.* 2010, Stengel & Taché, 2011). Nesfatin-1 expression in the nucleus ambiguus has been documented relatively recent (Goebel *et al.* 2009; Goebel-Stengel *et al.*, 2011). Given the key role of nucleus ambiguus in the autonomic cardiac regulation (Mendelowitz, 1999), we sought experimental evidence of a functional role of nesfatin-1 in cardiac-projecting neurons of nucleus ambiguus. Since we have previously found that nesfatin-1 elicits calcium signaling in neurons (Brailoiu *et al.* 2007), we first used calcium imaging to test the responsiveness of cardiac preganglionic neurons of nucleus ambiguus to nesfatin-1.

Treatment of cardiac vagal neurons with nesfatin-1 induced a rapid and dose-dependent rise in $[Ca^{2+}]_i$ in cardiac preganglionic neurons of nucleus ambiguus. The response pattern was similar to that identified in hypothalamic neurons (Brailoiu *et al.* 2007), and likely indicative of interaction with a G protein-coupled receptor. The amplitude of the Ca^{2+} response triggered by a second application of nesfatin-1 was lower than that of the first. This tachyphylactic response suggests receptor desensitization, a common phenomenon among G

protein-coupled receptors (Gainetdinov *et al.* 2004). However, tachyphylaxis did not occur, when nucleus ambiguus neurons were treated with urocortin 3 following the treatment with nesfatin-1. This may indicate the lack of heterologous sensitization between CRF₂ receptor, responsible for the Ca²⁺ response to urocortin 3 in nucleus ambiguus (Brailoiu *et al.* 2012), and the nesfatin-1 receptor.

While evidence of a specific nesfatin-1 receptor is lacking, studies with pharmacological antagonists suggest that the melanocortin system (Oh-I *et al.* 2006; Yosten & Samson 2009; Tanida & Mori 2011) or oxytocin system (Yosten & Samson 2010) play a role in the neural circuitry mediating the effects of nesfatin-1. For example, prior administration of the antagonist of the melanocortin receptor type 3/4, SHU9119 (Adan *et al.* 1999), eliminated the nesfatin-1-induced satiety in rats (Oh-I *et al.* 2006). However, treatment with the melanocortin receptor type 3/4 antagonist, SHU9110, or with the oxytocin receptor antagonist L-371,257 did not affect the nesfatin-1-induced increase in cytosolic Ca²⁺ in nucleus ambiguus neurons. Since the ability of oxytocin or melanocortin antagonists to block the effects of nesfatin-1 has been attributed to the sympatho-stimulatory action of the peptide in the nucleus of the tractus solitarius (NTS), the lack of effect of the antagonists noted here is not surprising.

We have previously demonstrated that in hypothalamic neurons, nesfatin-1-dependent Ca²⁺ response is pertussis toxin-sensitive, thus coupled with Gi/o proteins. In hypothalamic neurons, the effect was also depended on protein kinase A (Brailoiu *et al.* 2007), which is largely activated via Gs proteins, indicating that nesfatin-1 receptor may switch coupling between the two types of G proteins (Daaka *et al.* 1997). However, this is not the case in neurons of nucleus ambiguus examined in the current study, as the nesfatin-1-induced elevation of cytosolic Ca²⁺ was not sensitive to cholera toxin, an inhibitor of Gs-dependent signaling, but only to the Gi/o blocker pertussis toxin.

In an additional series of experiments we sought to identify the source of Ca²⁺ mobilized by nesfatin-1. In the absence of extracellular Ca²⁺, nesfatin-1 did not elicit a Ca²⁺ response in cardiac preganglionic neurons, suggesting the effect was dependent on Ca²⁺ influx but not on Ca²⁺ release from internal stores. Using selective inhibitors of plasmalemmal Ca²⁺ channels we show that Ca²⁺ entry in response to nesfatin-1 occurs largely through P/Q-type Ca²⁺ channels, while the N- and L-types have no significant contribution. In hypothalamic neurons, in addition to the P/Q-type Ca²⁺ current, we found a contribution of the L-type Ca²⁺ current to nesfatin-1-induced response (Brailoiu *et al.* 2007). However, the Ca²⁺ current in cardiac parasympathetic neurons of nucleus ambiguus is mediated nearly entirely by P/Q channels (Irnatien *et al.* 2003). Similar to nesfatin-1, urocortin 3 also activates P/Q Ca²⁺ channels in nucleus ambiguus neurons (Chitravanshi *et al.* 2012, Brailoiu *et al.* 2012).

A valuable finding of this study is that nesfatin-1 induced dose-dependent membrane depolarization of cardiac vagal neurons via a Gi/o-mediated mechanism, pointing to a physiological role of nesfatin-1 and its receptor in the nucleus ambiguus. We have previously found a good correlation between the membrane potential of nucleus ambiguus neurons measured with classical electrophysiological techniques in brainstem slices and with voltage-sensor dyes in cultured nucleus ambiguus neurons (Brailoiu *et al.* 2009).

Remarkably, nesfatin-1 depolarized NPY and NUCB2 neurons from NTS while producing heterogeneous effects (depolarization and hyperpolarization) in GABAergic neurons or those expressing MC₄ receptors (Mimee *et al.* 2012). Nesfatin-1-induced depolarization in NTS neurons was correlated with an increase in blood pressure and heart rate produced by microinjection of the peptide in medial NTS (Mimee *et al.* 2012). In addition, nesfatin-1 activates hypothalamic neurons and produces tachycardic and hypertensive response via sympathetic activation (Yosten and Samson, 2009).

Nesfatin-1 is synthesized both peripherally and in the central nervous system (Angelone *et al.* 2012, Oh-I *et al.* 2006) and crosses the blood-brain barrier by nonsaturable mechanisms (Pan *et al.* 2007, Price *et al.* 2007). Other peptides involved in hypothalamic control of appetite, such as orexin-A (Ciriello & de Oliveira 2003), neuropeptide Y (Gray *et al.* 2004) or α -melanocyte stimulating hormone (Chitravanshi *et al.* 2009) also activate the nucleus ambiguus neurons.

Given that activation of cardiac vagal neurons of nucleus ambiguus leads to release of acetylcholine to the heart and consequent bradycardia (Mendelowitz 1999) we next carried out *in vivo* studies and examined whether or not microinjection of nesfatin-1 into nucleus ambiguus affects the heart rate. Since anesthetics may impair the cardiovascular reflexes by acting on nucleus ambiguus neurons (Irnaten *et al.* 2002a, b) we monitored the heart rate by telemetry in conscious, freely moving rats. The biotelemetric measurement permits the monitoring of heart rate during the microinjection of a compound to be conducted in a stress-free manner. Stress-induced tachycardia is documented to occur as a consequence of animal handling (McDouglas *et al.* 2004). Microinjection of nesfatin-1 in nucleus ambiguus elicited bradycardia in conscious, freely moving rats. We also carried out heart rate and blood pressure measurements via tail-cuff method and identified a consistent bradycardic response elicited by L-glutamate and nesfatin-1 without a change in blood pressure. Similarly, previous studies indicated a very good correlation between telemetric and tail-cuff measurements of blood pressure and heart rate in rats (Fraser *et al.* 2001; Feng *et al.* 2008).

While previous studies indicate a modulatory effect of nesfatin-1 on sympathetic tone at central and peripheral levels (Yosten & Samson 2009, Tanida & Mori 2011), our results indicate for the first time that nesfatin-1 activates cardiac vagal neurons of nucleus ambiguus leading to a decrease in heart rate. Microinjection of nesfatin-1 intracerebroventricular (Yosten & Samson 2009; Tanida & Mori 2011) or in the medial NTS increases blood pressure and heart rate in conscious or anesthetized rats, supporting multiple sites of action for nesfatin-1 in autonomic cardiovascular control. Similarly, other peptides were reported to act at multiple levels, to modulate both parasympathetic and sympathetic tone. For example, orexins modulate the activity of CVNs of nucleus ambiguus (Dergacheva *et al.* 2005) and excite sympathetic neurons of rostral ventrolateral medulla (Huang *et al.* 2010) and of spinal cord (Antunes *et al.* 2001). In humans, oxytocin increases both sympathetic and parasympathetic cardiac activity (Norman *et al.* 2011). Moreover, oxytocin modulates cardiovascular activity by acting on NTS (Michelini, 2001) to facilitate vagal outflow (Higa *et al.* 2002) with implications for exercise-induced tachycardia (Braga *et al.* 2001). Arginine-vasopressin increases the GABAergic inhibitory transmission in nucleus ambiguus

(Wang *et al.* 2002) while acting as an excitatory transmitter in rostral ventrolateral medulla (Yang *et al.* 2001).

These reports indicate that peptides exert their modulatory effects on autonomic cardiovascular tone at multiple sites and via multiple mechanisms: recruitment of one mechanism or another may be dictated by physiological or pathophysiological conditions. Our results further support the complexity of nesfatin-1 signaling in the cardiovascular system. Since nesfatin-1 is one of the most potent anorexigenic peptides, further studies are needed to clarify whether or not nesfatin-1 plays any role in the bradycardia reported among patients suffering from anorexia nervosa (Portilla 2011).

Acknowledgments

This study was supported by NIH grants HL090804 (EB), HL105414 (DGT) and HL091096 and HL091799 (JER) from the Department of Health and Human Services.

References

- Angelone T, Filice E, Pasqua T, Amodio N, Galluccio M, Montesanti G, Quintieri AM, Cerra MC. Nesfatin-1 as a novel cardiac peptide: identification, functional characterization, and protection against ischemia/reperfusion injury. *Cell Mol Life Sci.* 2012; 70:495–509. [PubMed: 22955491]
- Adan RA, Szklarczyk AW, Oosterom J, Brakkee JH, Nijenhuis WA, Schaaper WM, Mueloen RH, Gispen WH. Characterization of melanocortin receptor ligands on cloned brain melanocortin receptors and on grooming behavior in the rat. *Eur J Pharmacol.* 1999; 378:249–258. [PubMed: 10493100]
- Benamar K, Addou S, Yondorf M, Geller EB, Eisenstein TK, Adler MW. Intrahypothalamic injection of the HIV-1 envelope glycoprotein induces fever via interaction with the chemokine system. *J Pharmacol Exp Ther.* 2010; 332:549–553. [PubMed: 19906780]
- Bouairi E, Kamendi H, Wang X, Gorini C, Mendelowitz D. Multiple types of GABAA receptors mediate inhibition in brain stem parasympathetic cardiac neurons in the nucleus ambiguus. *J Neurophysiol.* 2006; 96:3266–3272. [PubMed: 16914614]
- Braga DC, Mori E, Higa KT, Morris M, Michelini LC. Central oxytocin modulates exercise-induced tachycardia. *Am J Physiol Regul Integr Comp Physiol.* 2000; 278:R1474–1482. [PubMed: 10848513]
- Brailoiu GC, Dun SL, Brailoiu E, Inan S, Yang J, Chang JK, Dun NJ. Nesfatin-1: distribution and interaction with a G protein-coupled receptor in the rat brain. *Endocrinology.* 2007; 148:5088–5094. [PubMed: 17627999]
- Brailoiu GC, Brailoiu E, Parkesh R, Galione A, Churchill GC, Patel S, Dun NJ. NAADP-mediated channel ‘chatter’ in neurons of the rat medulla oblongata. *Biochem J.* 2009; 419:91–97. 92 p following 97. [PubMed: 19090786]
- Brailoiu GC, Gurzu B, Gao X, et al. Acidic NAADP-sensitive calcium stores in the endothelium: agonist-specific recruitment and role in regulating blood pressure. *J Biol Chem.* 2010; 285:37133–37137. [PubMed: 20876534]
- Brailoiu GC, Deliu E, Tica AA, Chitravanshi VC, Brailoiu E. Urocortin 3 elevates cytosolic calcium in nucleus ambiguus neurons. *J Neurochem.* 2012; 122:1129–1136. [PubMed: 22774996]
- Brailoiu GC, Arterburn JB, Oprea TI, Chitravanshi VC, Brailoiu E. Bradycardic effects mediated by activation of G protein-coupled estrogen receptor (GPER) in rat nucleus ambiguus. *Exp Physiol.* 2013; 98:679–691. [PubMed: 23104934]
- Brauner T, Hulser DF, Strasser RJ. Comparative measurements of membrane potentials with microelectrodes and voltage-sensitive dyes. *Biochim Biophys Acta.* 1984; 771:208–216. [PubMed: 6704395]

- Chitravanshi VC, Bhatt S, Sapru HN. Microinjections of alpha-melanocyte stimulating hormone into the nucleus ambiguus of the rat elicit vagally mediated bradycardia. *Am J Physiol Regul Integr Comp Physiol.* 2009; 296:R1402–1411. [PubMed: 19297540]
- Chitravanshi VC, Kawabe K, Sapru HN. Bradycardic effects of microinjections of urocortin 3 into the nucleus ambiguus of the rat. *Am J Physiol Regul Integr Comp Physiol.* 2012; 303:R1023–1030. [PubMed: 23019211]
- Ciriello J, de Oliveira CV. Cardiac effects of hypocretin-1 in nucleus ambiguus. *Am J Physiol Regul Integr Comp Physiol.* 2003; 284:R1611–1620. [PubMed: 12573979]
- Daaka Y, Luttrell LM, Lefkowitz RJ. Switching of the coupling of the beta2-adrenergic receptor to different G proteins by protein kinase A. *Nature.* 1997; 390:88–91. [PubMed: 9363896]
- Dergacheva O, Wang X, Huang ZG, Bouairi E, Stephens C, Gorini C, Mendelowitz D. Hypocretin-1 (orexin-A) facilitates inhibitory and diminishes excitatory synaptic pathways to cardiac vagal neurons in the nucleus ambiguus. *J Pharmacol Exp Ther.* 2005; 314:1322–1327. [PubMed: 15947034]
- Dergacheva O, Bateman R, Byrne P, Mendelowitz D. Orexinergic modulation of GABAergic neurotransmission to cardiac vagal neurons in the brain stem nucleus ambiguus changes during development. *Neuroscience.* 2012; 209:12–20. [PubMed: 22390944]
- Feng M, Whitesall S, Zhang Y, Beibel M, D'Alecy L, DiPetrillo K. Validation of volume-pressure recording tail-cuff blood pressure measurements. *Am J Hypertens.* 2008; 21:1288–1291. [PubMed: 18846043]
- Fraser TB, Turner SW, Mangos GJ, Ludbrook J, Whitworth JA. Comparison of telemetric and tail-cuff blood pressure monitoring in adrenocorticotrophic hormone-treated rats. *Clin Exp Pharmacol Physiol.* 2001; 28:831–835. [PubMed: 11553024]
- Gainetdinov RR, Premont RT, Bohn LM, Lefkowitz RJ, Caron MG. Desensitization of G protein-coupled receptors and neuronal functions. *Annu Rev Neurosci.* 2004; 27:107–144. [PubMed: 15217328]
- García-Galiano D, Navarro VM, Gaytan F, Tena-Sempere M. Expanding roles of NUCB2/nesfatin-1 in neuroendocrine regulation. *J Mol Endocrinol.* 2010; 45:281–290. [PubMed: 20682642]
- Goebel M, Stengel A, Wang L, Lambrecht NW, Tache Y. Nesfatin-1 immunoreactivity in rat brain and spinal cord autonomic nuclei. *Neurosci Lett.* 2009; 452:241–246. [PubMed: 19348732]
- Goebel-Stengel M, Wang L, Stengel A, Taché Y. Localization of nesfatin-1 neurons in the mouse brain and functional implication. *Brain Res.* 2011; 1396:20–34. [PubMed: 21555116]
- Gray AL, Johnson TA, Lauenstein JM, Newton SS, Ardell JL, Massari VJ. Parasympathetic control of the heart. III. Neuropeptide Y-immunoreactive nerve terminals synapse on three populations of negative chronotropic vagal preganglionic neurons. *J Appl Physiol.* 2004; 96:2279–2287. [PubMed: 14978003]
- Grynkiewicz G, Poenie M, Tsien RY. A new generation of Ca²⁺ indicators with greatly improved fluorescence properties. *J Biol Chem.* 1985; 260:3440–3450. [PubMed: 3838314]
- Higa KT, Mori E, Viana FF, Morris M, Michelini LC. Baroreflex control of heart rate by oxytocin in the solitary-vagal complex. *Am J Physiol Regul Integr Comp Physiol.* 2002; 282:R537–545. [PubMed: 11792664]
- Huang SC, Dai YW, Lee YH, Chiou LC, Hwang LL. Orexins depolarize rostral ventrolateral medulla neurons and increase arterial pressure and heart rate in rats mainly via orexin 2 receptors. *J Pharmacol Exp Ther.* 2010; 334:522–529. [PubMed: 20494957]
- Imaten M, Wang J, Chang KS, Andresen MC, Mendelowitz D. Ketamine inhibits sodium currents in identified cardiac parasympathetic neurons in nucleus ambiguus. *Anesthesiology.* 2002a; 96:659–666. [PubMed: 11873042]
- Imaten M, Wang J, Venkatesan P, Evans CK, Chang KS, Andresen MC, Mendelowitz D. Ketamine inhibits presynaptic and postsynaptic nicotinic excitation of identified cardiac parasympathetic neurons in nucleus ambiguus. *Anesthesiology.* 2002b; 96:667–674. [PubMed: 11873043]
- Imaten M, Aicher SA, Wang J, Venkatesan P, Evans C, Baxi S, Mendelowitz D. Mu-opioid receptors are located postsynaptically and endomorphin-1 inhibits voltage-gated calcium currents in premotor cardiac parasympathetic neurons in the rat nucleus ambiguus. *Neuroscience.* 2003; 116:573–582. [PubMed: 12559112]

- Kuo MS, Bock MG, Freidinger RM, Guidotti MT, Lis EV, Pawluczyk JM, Perlow DS, Pettibone DJ, Quigley AG, Reiss DR, Williams PD, Woyden CJ. Nonpeptide oxytocin antagonists: potent, orally bioavailable analogs of L-371,257 containing a 1-R-(pyridyl)ethyl ether terminus. *Bioorg Med Chem Lett.* 1998; 8:3081–3086. [PubMed: 9873680]
- Maejima Y, Sedbazar U, Suyama S, et al. Nesfatin-1-regulated oxytocinergic signaling in the paraventricular nucleus causes anorexia through a leptin-independent melanocortin pathway. *Cell Metab.* 2009; 10:355–365. [PubMed: 19883614]
- Mendelowitz D, Kunze DL. Identification and dissociation of cardiovascular neurons from the medulla for patch clamp analysis. *Neurosci Lett.* 1991; 132:217–221. [PubMed: 1784423]
- Mendelowitz D. Advances in Parasympathetic Control of Heart Rate and Cardiac Function. *News Physiol Sci.* 1999; 14:155–161. [PubMed: 11390842]
- McDougall SJ, Lawrence AJ, Widdop RE. Differential cardiovascular responses to stressors in hypertensive and normotensive rats. *Experimental Physiology.* 2005; 90:141–150. [PubMed: 15542615]
- Michelini LC. Oxytocin in the NTS. A new modulator of cardiovascular control during exercise. *Ann N Y Acad Sci.* 2001; 940:206–220. [PubMed: 11458679]
- Mimee A, Smith PM, Ferguson AV. Nesfatin-1 influences the excitability of neurons in the nucleus of the solitary tract and regulates cardiovascular function. *Am J Physiol Regul Integr Comp Physiol.* 2012; 302:R1297–1304. [PubMed: 22442196]
- Norman GJ, Cacioppo JT, Morris JS, Malarkey WB, Berntson GG, Devries AC. Oxytocin increases autonomic cardiac control: moderation by loneliness. *Biol Psychol.* 2011; 86:174–180. [PubMed: 21126557]
- Oh-I S, Shimizu H, Satoh T, Okada S, Adachi S, Inoue K, Eguchi H, Yamamoto M, Imaki T, Hashimoto K, Tsuchiya T, Monden T, Horiguchi K, Yamada M, Mori M. Identification of nesfatin-1 as a satiety molecule in the hypothalamus. *Nature.* 2006; 443:709–712. [PubMed: 17036007]
- Palasz A, Krzystanek M, Worthington J, Czajkowska B, Kostro K, Wiaderkiewicz R, Bajor G. Nesfatin-1, a unique regulatory neuropeptide of the brain. *Neuropeptides.* 2012; 46:105–112. [PubMed: 22225987]
- Pan W, Hsueh H, Kastin AJ. Nesfatin-1 crosses the blood-brain barrier without saturation. *Peptides.* 2007; 11:2223–2228. [PubMed: 17950952]
- Paxinos, G.; Watson, C. *The Rat Brain in Stereotaxic Coordinates.* 4. Academic Press; San Diego: 1998.
- Portilla MG. Bradycardia: an important physical finding in anorexia nervosa. *J Ark Med Soc.* 2011; 107:206–208. [PubMed: 21739848]
- Price TO, Samson WK, Niehoff ML, Banks WA. Permeability of the blood-brain barrier to a novel satiety molecule nesfatin-1. *Peptides.* 2007; 28:2372–2381. [PubMed: 18006117]
- Schoniger S, Wehming S, Gonzalez C, Schobitz K, Rodriguez E, Oksche A, Yulis CR, Nurnberger F. The dispersed cell culture as model for functional studies of the subcommissural organ: preparation and characterization of the culture system. *J Neurosci Methods.* 2001; 107:47–61. [PubMed: 11389941]
- Stengel A, Taché Y. Minireview: nesfatin-1--an emerging new player in the brain-gut, endocrine, and metabolic axis. *Endocrinology.* 2011; 152:4033–4038. [PubMed: 21862618]
- Tanida M, Mori M. Nesfatin-1 stimulates renal sympathetic nerve activity in rats. *Neuroreport.* 2011; 22:309–312. [PubMed: 21451359]
- Yamawaki H, Takahashi M, Mukohda M, Morita T, Okada M, Hara Y. A novel adipocytokine, nesfatin-1 modulates peripheral arterial contractility and blood pressure in rats. *Biochem Biophys Res Commun.* 2012; 418:676–681. [PubMed: 22293188]
- Yang Z, Bertram D, Coote JH. The role of glutamate and vasopressin in the excitation of RVL neurones by paraventricular neurones. *Brain Res.* 2001; 908:99–103. [PubMed: 11457436]
- Yosten GL, Samson WK. Nesfatin-1 exerts cardiovascular actions in brain: possible interaction with the central melanocortin system. *Am J Physiol Regul Integr Comp Physiol.* 2009; 297:R330–336. [PubMed: 19474390]

- Yosten GL, Samson WK. The anorexigenic and hypertensive effects of nesfatin-1 are reversed by pretreatment with an oxytocin receptor antagonist. *Am J Physiol Regul Integr Comp Physiol.* 2010; 298:R1642–1647. [PubMed: 20335376]
- Wang J, Irnaten M, Venkatesan P, Evans C, Mendelowitz D. Arginine vasopressin enhances GABAergic inhibition of cardiac parasympathetic neurons in the nucleus ambiguus. *Neuroscience.* 2002; 111:699–705. [PubMed: 12031355]

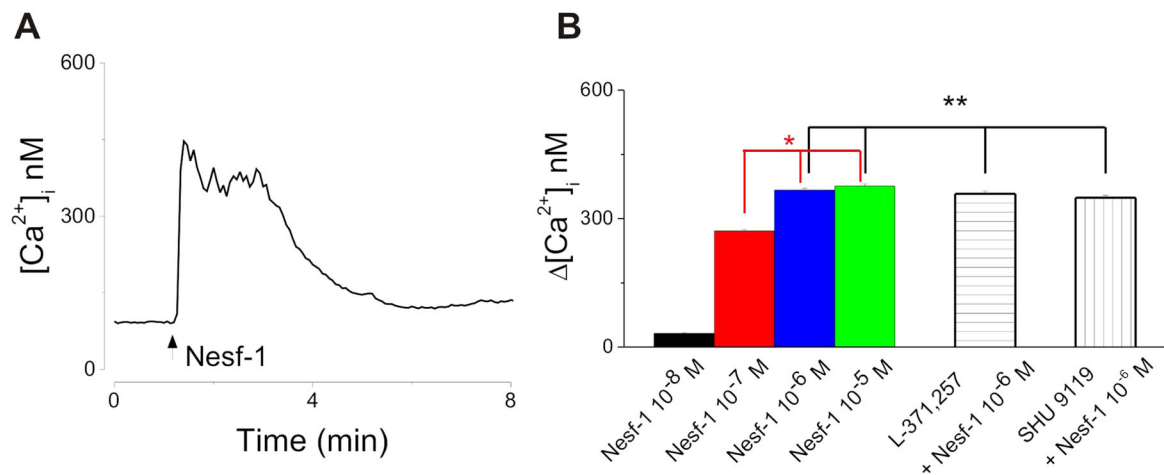


Figure 1. Nesfatin-1 elevates $[Ca^{2+}]_i$ in a dose-dependent manner in cardiac vagal preganglionic neurons of nucleus ambiguus

A, Representative recording of increase in $[Ca^{2+}]_i$ upon administration of 10^{-6} M nesfatin-1 (Nesf-1). **B**, Comparison of the Ca^{2+} responses elicited by increasing concentrations of nesfatin-1 (10^{-8} , 10^{-7} , 10^{-6} , and 10^{-5} M); and nesfatin-1 (10^{-6} M) in the presence of the oxytocin receptor antagonist, L-371,257 or of the antagonist of melanocortin receptors type 3/4, SHU 9119; * $P < 0.05$; ** $P > 0.05$.

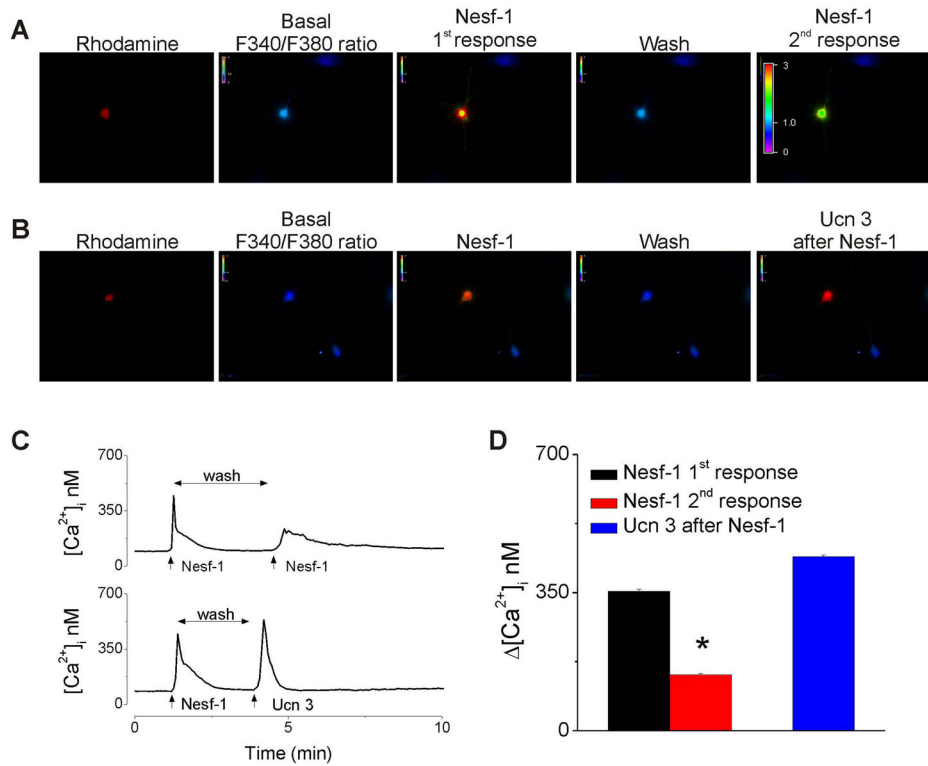


Figure 2. Nesfatin-1-induced Ca²⁺ response is subject to tachyphylaxis

A, Illustration of changes in fura-2 AM fluorescence ratio F340/380, before (basal) and during the first and second administration of nesfatin-1 (Nesf-1, 10⁻⁶M) in a rhodamine-labeled cardiac vagal neuron. **B**, Illustration of changes in F340/380 before (basal) and during the administration of nesfatin-1 (10⁻⁶ M) and urocortin 3 (Ucn 3, 10⁻⁶ M) in a rhodamine-labeled cardiac vagal neuron. **C**, Representative Ca²⁺ responses of nucleus ambiguus neurons to two consecutive administrations of nesfatin (10⁻⁶ M) or urocortin 3 (10⁻⁶ M) after nesfatin-1. **D**, Comparison of the amplitudes of [Ca²⁺]_i elevations produced by the first and second application of nesfatin-1 (10⁻⁶M), and by urocortin 3 (Ucn 3) after nesfatin **P* < 0.05.

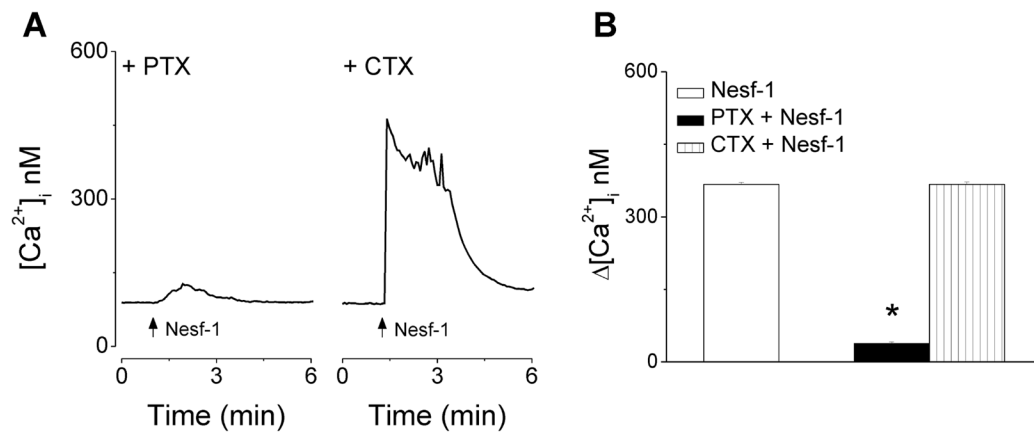


Figure 3. Nesfatin-1 activates a Gi/o-coupled receptor

A, Characteristic $[Ca^{2+}]_i$ recordings illustrating the responses of cardiac vagal neurons to administration of nesfatin-1 in presence of inhibitors of Gi/o- or Gs-dependent signaling (pertussis toxin, PTX, 100 nM and cholera toxin, CTX, 100 nM, respectively). **B**, Comparison of the Ca^{2+} responses elicited by nesfatin-1 application to cardiac preganglionic neurons in absence and presence of the indicated inhibitors; * $P < 0.05$.

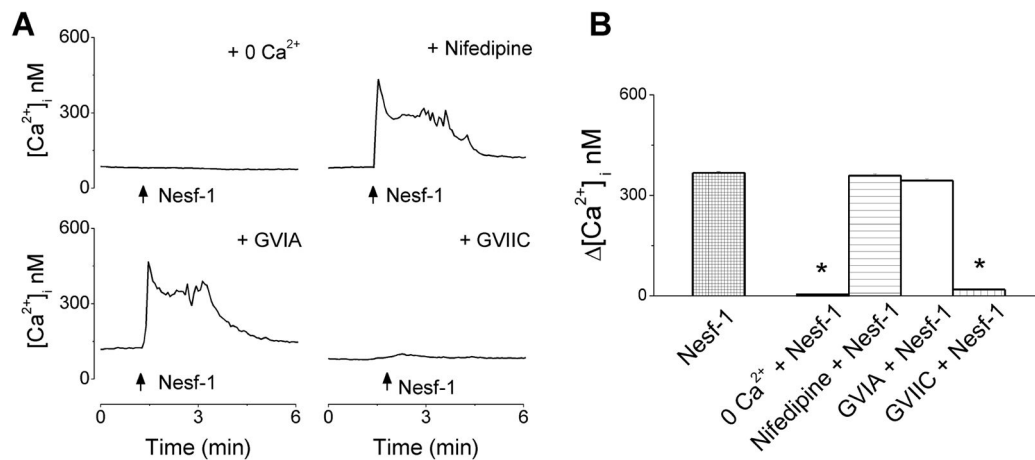


Figure 4. Nesfatin-1 promotes Ca^{2+} influx through P/Q-type voltage gated Ca^{2+} channels

A, Typical traces illustrating the Ca^{2+} responses of nucleus ambiguus neurons to nesfatin-1 (10^{-6} M) application in Ca^{2+} -free (top left panel) and Ca^{2+} -containing saline in presence of nifedipine (L-type Ca^{2+} channel blocker, $1\mu\text{M}$, top right), -conotoxin GVIA (GVIA, N-type Ca^{2+} channel blocker, 100 nM , bottom left) or ω -conotoxin MVIIC (MVIIC, P/Q-type Ca^{2+} channel blocker, 100 nM , bottom right). **B**, Comparison of the amplitudes of $[\text{Ca}^{2+}]_i$ increases produced by nesfatin-1 in the indicated conditions; * $P < 0.05$.

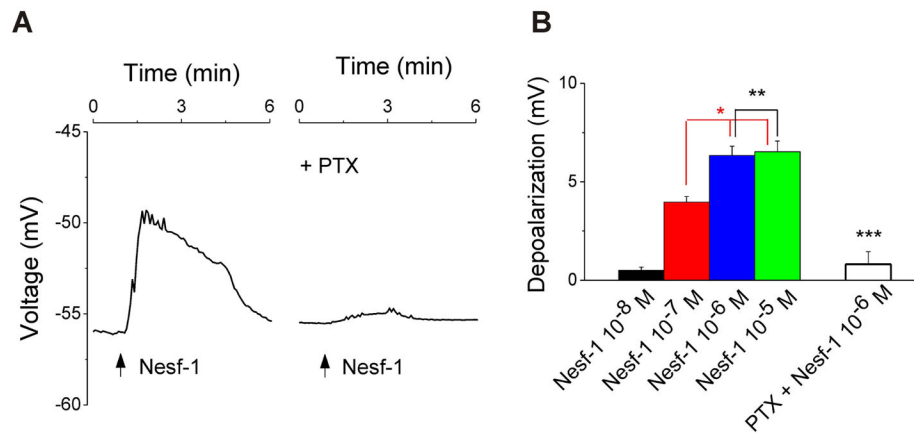


Figure 5. Nesfatin-1 elicits Gi/o-dependent depolarization of cardiac preganglionic neurons of nucleus ambiguus

A, Representative recordings illustrating changes in membrane potential of cardiac vagal neurons upon application of nesfatin-1 (10^{-6} M) in absence (left) and presence of Gi/o inhibitor pertussis toxin (PTX, 100 nM, right). **B**, Nesfatin-1 (10^{-8} , 10^{-7} , 10^{-6} and 10^{-5} M) produces a concentration-dependent depolarization of nucleus ambiguus neurons. The response to 10^{-6} M nesfatin-1 is sensitive to Gi/o blockade with PTX (100 nM); $P < 0.05$ compared to basal (*), or to 10^{-6} M nesfatin-1 (***) ($P > 0.05$ (**)).

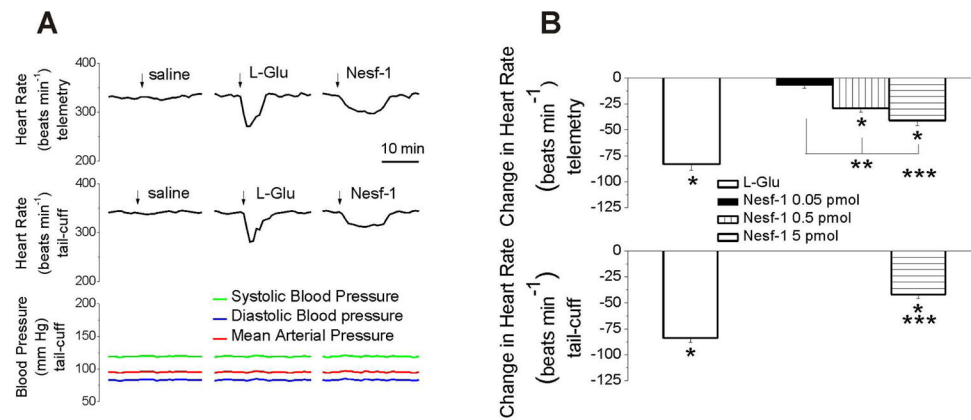


Figure 6. Microinjection of nesfatin-1 into the nucleus ambiguus elicits bradycardia in conscious rats

A, Representative examples of heart rate and blood pressure recordings after microinjection of saline, L-glutamate (L-Glu, 5 mM, 50 nl) and nesfatin-1 (Nesf-1, 5 pmol, 50 nl) via telemetry (top trace) or tail-cuff method (bottom traces). **B**, Microinjection of nesfatin-1 (0.05, 0.5, and 5 pmol) produced a dose-dependent decrease in heart rate. Microinjection of L-glutamate (L-Glu, 5 mM, 50 nl) and nesfatin-1 (5 pmol, 50 nl) produced a similar decrease in heart rate in rats when tail-cuff method was used as compared to telemetry. * $P < 0.05$ as compared to basal heart rate (*); ** $P < 0.05$ as compared to the other treatment groups (**); *** $P > 0.05$ as compared to the effect of nesfatin-1 on heart rate monitored via telemetry vs tail-cuff.